# Optimization of the size of UPQC system based on data-driven control design

Ye, Jian; Gooi, Hoay Beng; Wu, Fengjiang

2018

Ye, J., Gooi, H. B., & Wu, F. (2018). Optimization of the size of UPQC system based on data-driven control design. IEEE Transactions on Smart Grid, 9(4), 2999-3008. doi:10.1109/TSG.2016.2624273

https://hdl.handle.net/10356/82864

https://doi.org/10.1109/TSG.2016.2624273

# Optimization of the Size of UPQC System Based on Data-Driven Control Design

Jian Ye, *Student Member, IEEE*, H. B. Gooi, *Senior Member, IEEE*, and Fengjiang Wu, *Member, IEEE*

***Abstract*—The unified power quality conditioner (UPQC) has become the most attractive solution to improve the power quality (PQ) in the microgrids. However, the high manufacturing cost is a huge challenge of popularizing the UPQC system. This paper investigates the optimal size of the UPQC system based on the compensation requirements. A generalized strategy is proposed to optimize the size of the UPQC system, which determines the fundamental ratings of the shunt converter, series converter, and series transformer. A data-driven control (DDC) based controller is developed using the variable phase angle control (PAC) method to realize the implementation of the designed UPQC system under the different compensating conditions. Moreover, the MATLAB and OPAL-RT simulation results validate the practicability of the generalized strategy and the DDC based controller.**

***Index Terms*—Unified power quality conditioner (UPQC), voltage sag and swell, volt-ampere (VA) optimization, phase angle control (PAC) method, data-driven control (DDC).**

## I. INTRODUCTION

IT IS well known that the unbalanced voltages, voltage swell and sag are the most general utility voltage quality problems [1], [2]. These problems will result in disruption of critical loads, bringing about substantial financial losses, degrading the power quality (PQ) and also lower the power factor of the system. It is important to maintain the PQ of the supply within the strict standards in the modern power system [3]-[6].

In 1998, Fujita and Akagi [7] proposed the Unified Power Quality Conditioner (UPQC) system which has the capability of improving PQ at both the source side and load side as shown in Fig. 1. The UPQC system contains two major parts, one is the power electronic converters where the series and shunt converters are integrated together, and the other one is the series transformer which handles the series injected voltage. Since then, UPQC has become one of the most attractive solution to improve PQ in the distribution system due to its superior performance in mitigating almost all major PQ problems [8]. In recent years, researchers start to investigate the applications of UPQC in smart grids [9]-[11]. However, UPQC is still at the research stage, which has not been widely utilized so far. The reason is that the UPQC system contains two sets of power converters and a transformer. This significantly increases the cost of producing and marketing the system. It is important to reduce the rating of the UPQC system without any compromise of the compensating capabilities. In this manner, it increases the utilization of the UPQC and reduces the cost of the system, which leads to high competitiveness of the whole system.

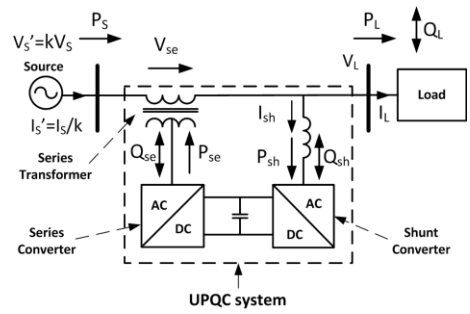


Fig. 1. UPQC general block diagram configuration.

Recently, several different methods [12]-[19] have been used to minimize the total VA loading of UPQC. In [12]-[19], it is noticed that the minimization of the total VA loading under a certain condition is realized by increasing the size of the UPQC.

In fact, the optimization of the size of the UPQC system has seldom been studied so far. There is no generalized strategy to optimize the rating of a UPQC system. The authors of [20] propose an algorithm to reduce the VA ratings of both the converters of UPQC. The minimization is based on the relationship between the VA loadings of UPQC and the displacement angle [21], [22]. The optimized VA ratings of both the converters are identified at a fixed displacement angle ($\delta = 15°$). By maintaining the fixed angle, both the converters VA loadings are below their ratings at any operating condition [20]. However, the rating of the transformer and those of the converters will affect each other. If the rating of the transformer is not considered during the optimization, the optimal VA ratings of the UPQC system cannot be achieved. In this paper, both the VA rating of the converter and that of the series transformer are taken care of during the optimization process. Furthermore, we are not limited to a fixed displacement angle to calculate the VA ratings. The variable phase angle control (PAC) method [21], [22] is applied in the proposed generalized

This work was supported by the Energy Innovation Programme Office (EIPO) through the National Research Foundation and Singapore Economic Development Board.

J. YE and H. B. Gooi are with the School of Electrical and Electronic Engineering, Nanyang Technological University, Singapore (e-mail: JYE007@e.ntu.edu.sg; EHBGOOI@ntu.edu.sg).

F. J. WU is with the School of Electrical and Electronic Engineering, Nanyang Technological University, Singapore 639798. He is currently on leave from the Department of Electrical Engineering, Harbin Institute of Technology, Harbin, China 150001 (e-mail: shimeng@hit.edu.cn).

strategy to reduce the VA rating of the UPQC system.

This paper investigates the optimal size of the whole UPQC system based on the compensation requirements. A generalized strategy is proposed to optimize the size of the UPQC system which determines the fundamental VA ratings of the shunt converter, series converter, and series transformer. The proposed UPQC system is compared with the UPQC-P, UPQC-$VA_{min}$, and UPQC in [20]. A data-driven control (DDC) [23], [24] based controller is developed to realize the implementation of the proposed UPQC system under the different compensating conditions. In recent years, the DDC approaches have been implemented in different fields, such as microgrids [25], heat exchanging process [26], fuel cell [27], and so on. One of the attractive features of the DDC approaches is that it is model-free control, which only requires the measured I/O data from the controlled system [23]. In the DDC approaches, the plant model disappears or no longer dominates the control process. Another feature of the DDC approaches is its high robustness [23]. If some parameters of the model, such as the impedances of inductors and capacitors are deviated from the original values due to aging, the model-based control (MBC) cannot maintain its stability. The reason is that the MBC requires the precise model of the controlled system. The DDC has stronger robustness regarding the model parameters changing caused by aging. Based on the developed DDC controller, the simulation study of the proposed UPQC system is also conducted in this paper.

## II. Problem Formulation

### A. Mathematical Modelling

The detailed phasor diagram of PAC with any arbitrary displacement angle ($\delta$) is illustrated in Fig. 2 [21], [22], where $V_S$ is the rated source voltage and $k$ is the source voltage ratio. $k$ represents the steady state, voltage sag, and voltage swell conditions when $k = 1$, $k < 1$, and $k > 1$ respectively. The series voltage ($V_{se}$) is injected with the proper phase angle ($\gamma$) and magnitude to maintain the resultant load voltage ($V_L$) at the rated value and a displacement angle ($\delta$) shift. For better demonstration, the steady state currents, i.e., load current ($I_L$) and shunt current ($I_{sh}$), in the conventional UPQC-P approach are presented with dotted lines in Fig. 2.

It is noted that the resulting load current ($I_L'$) has an angle ($\delta$) shift according to the displacement angle ($\delta$) [21], [22]. Therefore, the load power factor angle ($\emptyset$) and the magnitude of the load current ($I_L$ or $I_L'$) are constant during operations. Based on the equations derived in [21], [22], we can establish the mathematical model of the UPQC system.

The magnitude of the series voltage is computed as follows:

$$V_{se} = V_S \cdot \sqrt{1 + k^2 - 2k\cos\delta} \tag{1}$$

The VA loading of the series converter can be determined as

$$S_{se} = V_{se} \cdot I_S^{'} = P_L \cdot \frac{1}{k} \cdot \sqrt{1 + k^2 - 2k\cos\delta} \tag{2}$$

The VA loading of the shunt converter can be expressed as

$$S_{sh} = \sqrt{P_{sh}^{\ 2} + Q_{sh}^{\ 2}} \tag{3}$$

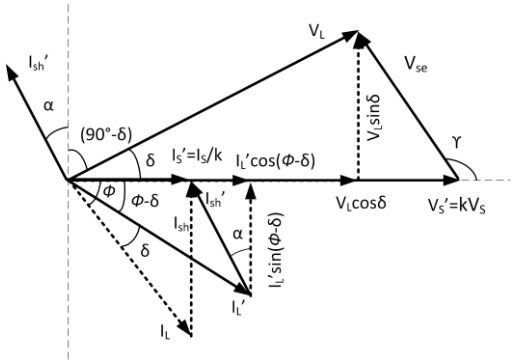


Fig. 2. The detailed phasor diagram of PAC [21], [22].

$$S_{sh} = \sqrt{P_L^{\ 2} \cdot \frac{1 + k^2 - 2k\cos\delta}{k^2} + Q_L^{\ 2} - 2Q_L P_L \cdot \frac{sin\delta}{k}} \tag{4}$$

Adding (2) and (4), the VA loading of UPQC is obtained as

$$S_{UPQC} = S_{se} + S_{sh} \tag{5}$$

The VA rating of the series transformer is calculated by multiplying the maximum winding current by the maximum series voltage as

$$S_{ST} = \max\left(V_{se}\right) \cdot \frac{I_S}{k_{min}} \tag{6}$$

All the aforementioned equations (1)-(6) are functions of $\delta$ and $k$.

### B. Objective Functions and Constraints

The main objective of this paper is to minimize the VA ratings of the whole system. The basic logic is that the VA loadings should not exceed the VA ratings. Based on the mathematical model and the basic logic, we formulate the optimization problem as follows

$$\text{min.} \quad F = (X, Y, Z) \tag{7}$$

$$\text{subject to} \quad S_{se}(k, \delta) \le X \tag{8}$$

$$S_{sh}(k, \delta) \le Y \tag{9}$$

$$V_{se}(k, \delta) \cdot \frac{I_S}{k_{\min}} \le Z \tag{10}$$

where in the objective function (7), $X$, $Y$, and $Z$ are the VA ratings of the series converter, shunt converter, and series transformer. The inequality constraints (8)-(10) can ensure that the VA loadings are within the limit of the VA ratings. After that, we introduce the weights in the objective functions [28]. In this work, the weights have physical meanings which are the unit costs of the transformer and converter. Then the physical meaning of the objective function turns out to be the total capital cost of the UPQC system. The optimization problem is rewritten as follows:

$$\text{min.} \quad \lambda^T F = \lambda_{in} \times (X + Y) + \lambda_{tr} \times Z \tag{11}$$

$$\text{subject to} \quad S_{se}(k_{\min}, \delta_1) \le X \tag{12}$$

$$S_{sh}(k_{\min}, \delta_1) \le Y \tag{13}$$

$$V_{se}(k_{\min}, \delta_1) \cdot \frac{I_S}{k_{\min}} \le Z \tag{14}$$

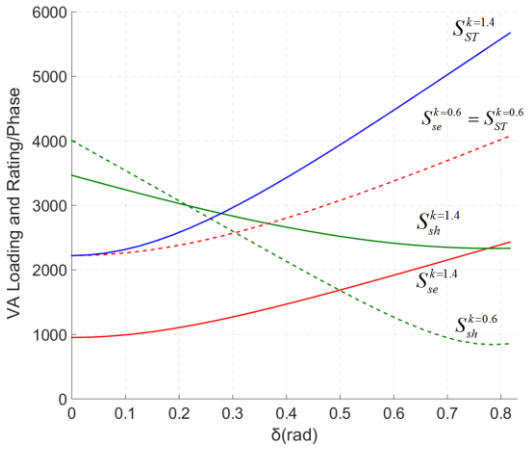


Fig. 3. VA loading curves of the series and shunt converters and VA rating curves of the series transformer for $k = 0.6$ and $k = 1.4$.

$$S_{se}(k_{\max}, \delta_2) \le X \tag{15}$$

$$S_{sh}(k_{\max}, \delta_2) \le Y \tag{16}$$

$$V_{se}(k_{\max}, \delta_2) \cdot \frac{I_S}{k_{\min}} \le Z \tag{17}$$

where in the objective function (11), $\lambda_{in}$ and $\lambda_{tr}$ are the unit costs of the converter and transformer; and $\lambda^T F$ is the total capital cost of the UPQC system. In (12)-(17), we only consider the worst-case scenario ($k = k_{min}$ and $k_{max}$) to reduce the computation burden of the problem. It is noted that the operating displacement angles are different under the two conditions. The worst-case scenario consideration ensures that the UPQC system will satisfy the worst compensating requirement. Based on (11)-(17), a generalized strategy is proposed to serve the purpose of minimizing the total capital cost of the UPQC system in the next section.

## III. DESIGN OF THE UPQC SYSTEM

### A. Search Strategy

To illustrate the process of finding the optimal point, we make the physical interpretation by considering the specific case in [20]. The source voltage is balanced and pure sinusoidal. The load is assumed to be balanced, harmonic-free, and inductive. The supply voltage is three-phase, $400\,V$ (line voltage), and $50\,Hz$. The full load power demand is $10\,kW + j10\,kvar$. The UPQC system is designed to have the capability of compensating 40% voltage swell and sag. The feasible operating displacement angle is in the range of $[0, \pi/4] rad$.

The VA loading curves of the series and shunt converters under the worst voltage sag and swell conditions ($k = 0.6$ and $k = 1.4$) are plotted in Fig. 3 using (2) and (4). The corresponding curves of the series transformer VA rating are also plotted in Fig. 3 using (6). The VA loading curve of the series converter and the VA rating curve of the series transformer for $k = 0.6$ are the same according to (2) and (6). It is noted that $S_{se}$, $S_{sh}$, and $S_{ST}$ are smooth nonlinear functions of $\delta$. The optimization problem is recognized as a smooth nonlinear programming (NLP), which can be solved by the NLP method, such as the interior-point method [29]. We rewrite the optimization problem as follows:

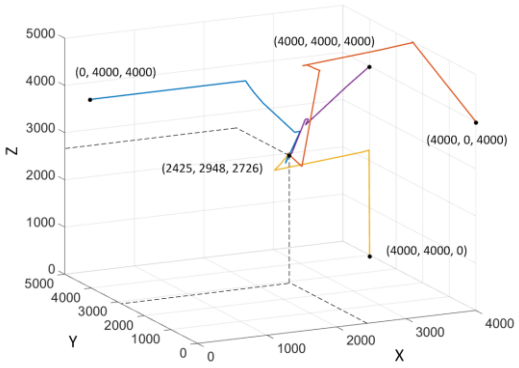


Fig. 4. Paths of four different initial points moving to the optimal point after iterations.

TABLE I
PSEUDO CODE

**Given** the starting point $x^0$, $t := t^0$, $\mu > 1$, tolerance $\varepsilon > 0$.
**Repeat** (until $m/t < \varepsilon$)
1. Centering. Starting at current $x$, use the Newton's method to compute $x^*(t)$ by minimizing $f_0 + (1/t) \cdot \phi$.
2. Update $x := x^*(t)$.
3. Increase $t := \mu t$.

$$\text{min.} \quad f_0(x) \tag{18}$$

$$\text{subject to} \quad f_i(x) \le 0, \quad i = 1, \ldots \tag{19}$$

where $x$ contains five variables, i.e., ($X$, $Y$, $Z$, $\delta_1$, $\delta_2$). In (19), $f_i(x) \le 0$ represents the six inequality constraints, hence, $m = 6$. The logarithmic barrier function of (19) is given by

$$\phi(x) = -\sum_{i=1}^{m} \log(-f_i(x)), \quad \text{dom}\phi = \{x \mid f_i \le 0\} \tag{20}$$

The optimization problem can be approximated via the logarithmic barrier function as

$$\text{min.} \quad f_0(x) + (1/t) \cdot \phi(x) \tag{21}$$

where the approximation improves as $t \to \infty$ in (21). We predefine $x^*(t)$ as the solution of (21), which is unique for each $t > 0$. The pseudo code is presented in Table I.

### B. Design of the UPQC

In this section, the UPQC is designed for the aforementioned specific case using the proposed generalized strategy. Input the load power demand ($P_L = 10kW$ and $Q_L = 10kvar$), rated line to line voltage ($V_L = 400V$) of the load, voltage compensating requirements ($k_{min} = 0.6$ and $k_{max} = 1.4$), unit cost of the converter and transformer ($\lambda_{in} = \$1.5/VA$ and $\lambda_{tr} = \$0.5/VA$), $t^0 = 1$, $\mu = 10$, and $\varepsilon = 1e^{-6}$ at the start of the algorithm. All the input data can be updated according to the practical situations in different systems. Moreover, a multi-start strategy is utilized to verify the calculated optimal point is a global one. We start with four different initial points (0, 4000, 4000, 0, 0), (4000, 0, 4000, 0, 0), (4000, 4000, 0, 0, 0), and (4000, 4000, 4000, 0, 0). The interior-point algorithm provably converges to the same optimal point (2425, 2948, 2726) as illustrated in Fig. 4. The optimization results of $X$, $Y$, and $Z$ are rounded. The optimal values of $\delta_1$ and $\delta_2$ are 0.23 and 0.24,

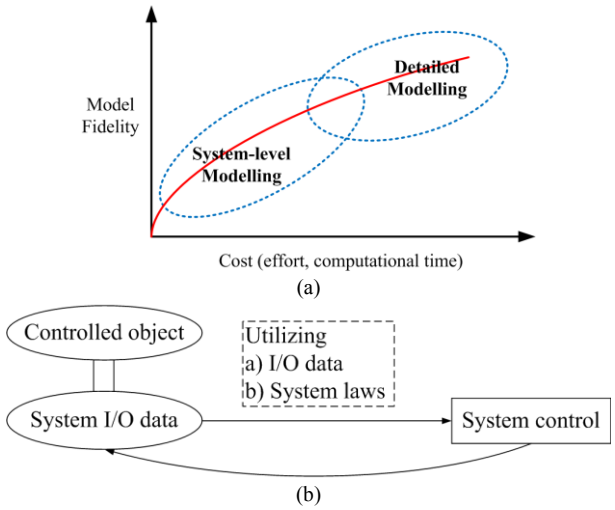


Fig. 5. The concept of the DDC approaches (a) model fidelity VS cost (b) architecture.

respectively. The optimal value of the objective function (11) is determined as 9423. Hence, the per-phase VA ratings of the series converter, shunt converter, and series transformer are determined as $2{,}425\,VA$, $2{,}948\,VA$, and $2{,}726\,VA$. The displacement angles under 40% voltage sag and swell are $0.23\,rad$ and $0.24\,rad$ respectively. The per-phase minimum capital cost of the UPQC system is \$9,423. The maximum series injected voltage is calculated as $113\,V$ using (6).

### C. Comparison Analysis

The VA rating of UPQC with the UPQC-P and UPQC-$VA_{min}$ approaches can be obtained by following the procedures and techniques in [12]-[20]. The comparison of UPQC with the different approaches is made in Table II. It is noted that UPQC-$VA_{min}$ increases the total capital cost significantly compared with that of UPQC-P. The proposed UPQC can reduce the total capital cost effectively by \$3,123, which is almost 10% of the original cost ($\$3{,}123/\$31{,}391 = 9.9\%$). The UPQC in [20] cannot provide the lowest total capital cost. This is because the authors in [20] did not consider the series transformer VA rating in the optimization process, and its capital cost was not involved. The designed UPQC in [20] was based on a fixed displacement angle ($\delta = 15^{\circ}$). However, the displacement angle in the proposed generalized strategy can be varied to obtain a lower total capital cost. To realize the implementation of the designed UPQC system, the corresponding control method is utilized.

## IV. PROPOSED DATA-DRIVEN CONTROL

This paper investigates the VA loadings of the UPQC system. The power coordination between both the converters should be taken care of for the UPQC. Hence, the controller should be developed from the viewpoint of the power. In this section, the DDC is developed to realize the implementation of the designed UPQC system. We first illustrate the relation between the model fidelity and cost in Fig. 5(a). The detailed modelling of the system requires a high cost, including the cost of effort and computational time. However, the system-level

TABLE II
TOTAL CAPITAL COST COMPARISON BETWEEN UPQC-P, UPQC-$VA_{MIN}$, UPQC IN [20], AND PROPOSED UPQC FOR THE SAME COMPENSATION REQUIREMENT

| UPQC Type | -P | -$VA_{min}$ | in [20] | Proposed UPQC |
|---|---|---|---|---|
| $S_{se}$/ph (VA) | 2,223 | 3,577 | 2,490 | 2,425 |
| $S_{sh}$/ph (VA) | 4,007 | 3,334 | 2,907 | 2,948 |
| $S_{ST}$/ph (VA) | 2,237 | 3,584 | 2,815 | 2,726 |
| $V_{se}$ (V) | 93 | 149 | 117 | 113 |
| Total Capital Cost/3-ph (\$) | 31,391 | 36,476 | 28,509 | 28,268 |
| Change in Total Capital Cost (\$) | 0 | +5,085 | −2,882 | −3,123 |

modelling requires a smaller cost. The MBC is based on the detailed modelling, while the DDC is based on the system-level modelling. The architecture of the DDC approaches is illustrated in Fig. 5(b). The I/O data is first measured from the controlled system. Then the system control is realized by utilizing the measured I/O data and system laws. In the proposed DDC, the measured I/O data is the source voltage $v_{S,abc}$, load voltage $v_{L,abc}$, source current $i_{S,abc}$, load current $i_{L,abc}$, and dc-link voltage $V_{dc}$. By using the power coordination laws described in Section II.A, the UPQC is controlled at system level. The proposed DDC can minimize the total online VA loading of UPQC and ensure that the VA loadings of the converters are within their ratings by coordinating the power between the series and shunt converters.

### A. Determination of the Instantaneous Power and Displacement Angle

The determination of the instantaneous power and displacement angle requires the measured source voltage $v_{S,abc}$, load voltage $v_{L,abc}$, and load current $i_{L,abc}$. The signal flow graph is presented in Fig. 6(a). The measured $v_{L,abc}$ and $i_{L,abc}$ are transformed from the $abc$ frame to the $\alpha\beta$ frame. By applying Akagi's instantaneous power (p-q) theory [30], the instantaneous load active and reactive power is computed using the $\alpha\beta$ components of the load current and voltage as follows

$$p = v_{L,\alpha}\cdot i_{L,\alpha} + v_{L,\beta}\cdot i_{L,\beta} \tag{22}$$

$$q = v_{L,\beta}\cdot i_{L,\alpha} - v_{L,\alpha}\cdot i_{L,\beta} \tag{23}$$

Meanwhile, the magnitude of the source voltage $|V_S|$ is obtained by measuring the fundamental peak value of the measured $v_{S,abc}$. The instantaneous value of the compensating requirement $k$ is calculated by dividing $|V_S|$ by the rated source voltage magnitude $V_S$. Based on the computed $p$, $q$, and $k$, the online VA loading optimization techniques will coordinate the power between the series and shunt converters by solving a NLP to give a corresponding displacement angle $\delta$ as follows

$$\text{min.} \quad S_{UPQC}(p,q,k,\delta) \tag{24}$$

$$\text{subject to} \quad S_{se}(p,k,\delta) \le S_{se\_O} \tag{25}$$

$$S_{sh}(p,q,k,\delta) \le S_{sh\_O} \tag{26}$$

$$V_{se}(k,\delta) \le V_{se\_O} \tag{27}$$

where in (24), $S_{UPQC}$ is the objective function from (5). In (25)-(27), the series injected voltage ($V_{se}$) and the operating VA

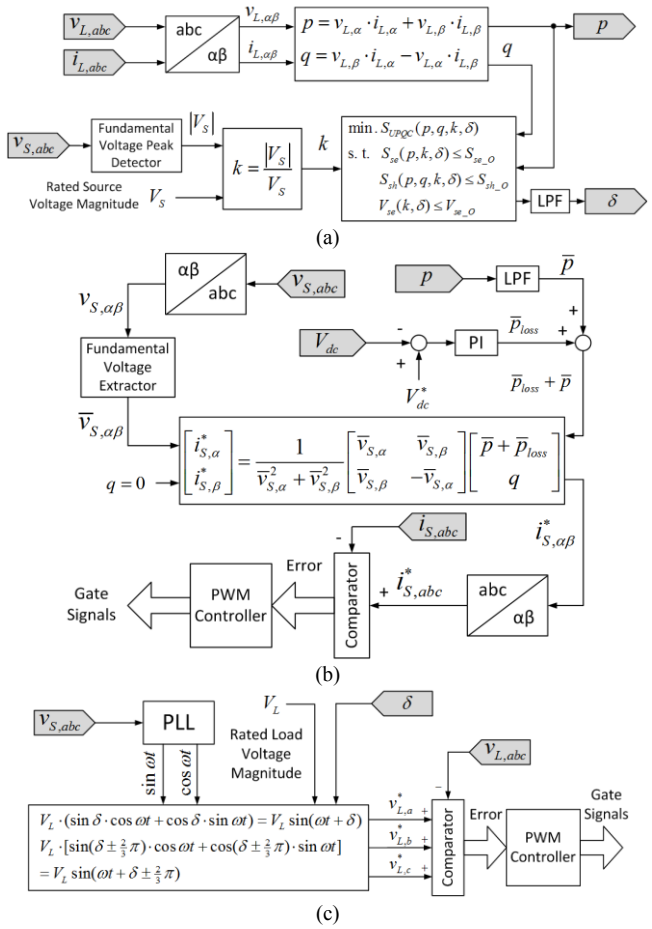


Fig. 6. Signal flow graphs (a) determination of the instantaneous power and displacement angle, (b) source current and dc-link control, (c) load voltage control.

loading of the series converter ($S_{se}$) and shunt converter ($S_{sh}$) are constrained to the rated values, i.e., $V_{se\_O}$, $S_{se\_O}$, and $S_{sh\_O}$. For each compensating requirement ($k$), the minimum VA loading ($S_{UPQC\_min}$) of UPQC and the corresponding operating displacement angle ($\delta$) are obtained by minimizing $S_{UPQC}$. It is noted that a low pass filter (LPF) is utilized to avoid rapid change in the magnitude of $\delta$.

### B. Source Current and dc-link Control

The control of the source current and dc-link requires the measured source voltage $v_{S,abc}$, source current $i_{S,abc}$, dc-link voltage $V_{dc}$, and calculated load active power $p$. Compared with the original p-q theory, we made a modification by generating the reference source current instead of the shunt compensating current. The LPF is used to generate the fundamental load active power $\overline{p}$. The error between the measured and reference dc-link capacitor voltage is processed by a proportional integral (PI) controller to generate the power loss ($\overline{p}_{loss}$) associated with the dc-link voltage supply. As the source will only supply the dc-link capacitor related power loss and the fundamental active power, $\overline{p}+\overline{p}_{loss}$ and $q=0$ are used to calculate the $\alpha\beta$ components of the reference source current. It is an inverse process of calculating the power, given by

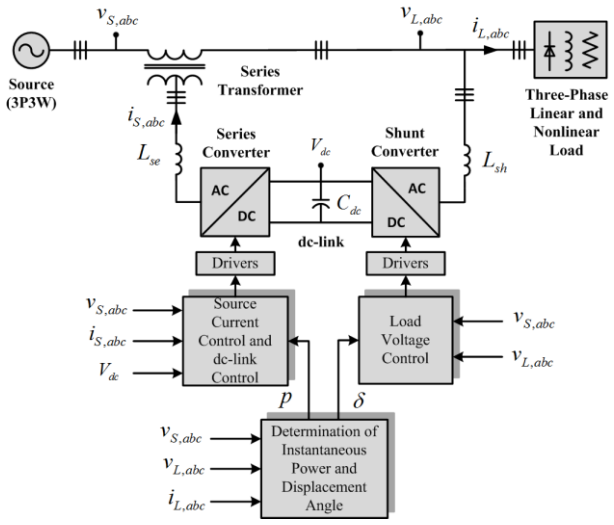


Fig. 7. Schematic of the DDC for the proposed UPQC.

$$\begin{bmatrix} i^*_{S,\alpha} \\ i^*_{S,\beta} \end{bmatrix} = \frac{1}{\overline{v}^2_{S,\alpha}+\overline{v}^2_{S,\beta}} \begin{bmatrix} \overline{v}_{S,\alpha} & \overline{v}_{S,\beta} \\ \overline{v}_{S,\beta} & -\overline{v}_{S,\alpha} \end{bmatrix} \begin{bmatrix} \overline{p}+\overline{p}_{loss} \\ q \end{bmatrix} \quad (28)$$

where in (28), $\overline{v}_{S,\alpha\beta}$ is obtained by extracting the fundamental voltage from the $\alpha\beta$ components of the $v_{S,abc}$. Then, the reference source current $i^*_{S,\alpha\beta}$ is transformed from the $\alpha\beta$ frame to the $abc$ frame. The error signal of the measured and reference source current is handled by the PWM controller to generate the switching signals. The signal flow graph is shown in Fig. 6(b).

### C. Load Voltage Control

The control of the load voltage requires the measured source voltage $v_{S,abc}$, load voltage $v_{L,abc}$, and calculated displacement angle $\delta$. The block diagram is presented in Fig. 6(c). A phase locked loop (PLL) controller is used to generate the $sin\omega t$ and $cos\omega t$ signals from $v_{S,abc}$. After that, $\delta$, $sin\omega t$, $cos\omega t$, and the rated load voltage magnitude $V_L$ are utilized to generate the reference load voltage $v^*_{L,abc}$. The error signal of the measured and reference load voltage is handled by the PWM controller to generate the switching signals.

### D. Dual Control Strategy

The dual control strategy [31] is applied for the proposed UPQC system. The schematic is illustrated in Fig. 7. In the dual control strategy, the load voltage control signals are sent to the shunt converter, where the shunt converter is operated as a sinusoidal voltage source. On the other hand, the source current and dc-link control signals are sent to the series converter, where the series converter is operated as a sinusoidal current source. The advantages of the dual control strategy are as follows

1) As the objective of the UPQC system is to maintain the desired source current and load voltage, the dual control strategy directly utilizes the reference source current and load voltage instead of the reference shunt compensating current and series injected voltage. This makes it a straightforward process from implementing the control to

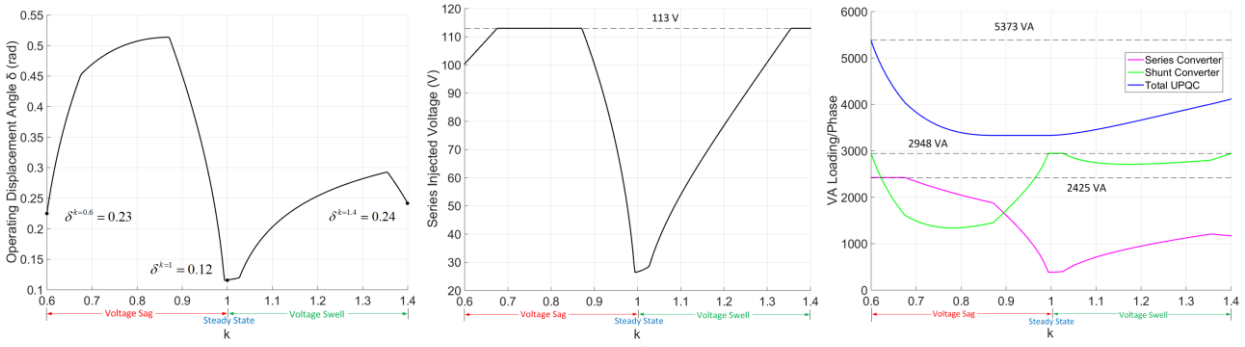


(a) (b) (c)

Fig. 8. Matlab simulation results of the proposed UPQC (a) displacement angle δ, (b) series transformer injected voltage $v_{se}$,and (c) per-phase VA loading of the series converter, shunt converter and total UPQC ($S_{se}$, $S_{sh}$, and $S_{UPQC}$).

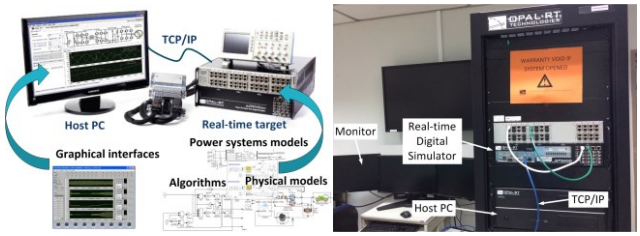


(a) (b)

Fig. 9. Real-time simulation (a) conceptual structure (b) OPAL-RT setup.

achieving the objective.

2) The dual control strategy is able to help the applied algorithms for reduction of complexity in the control scheme.

The process of the proposed DDC approach is summarized as follows:

1) The I/O data is first measured from the controlled UPQC system.
2) Based on the measured I/O data, the instantaneous power ($p$,$q$) and displacement angle ($\delta$) are computed by solving the Akagi's p-q equations and the NLP problem stated in Section IV.A, respectively.
3) The $p$ and $\delta$ are used to generate the reference source current and load voltage, respectively.
4) The reference source current and load voltage signals are sent to the series and shunt converters respectively to realize the control of the UPQC system.

## V. MATLAB SIMULATION RESULTS

The simulation of the designed UPQC is conducted using the MATLAB platform. The simulation results are illustrated in Fig. 8. It is noted that the simulation of the designed UPQC is conducted for all compensating conditions from 40% voltage sag ($k = 0.6$) to 40% voltage swell ($k = 1.4$) under the full load ($10\ kW + j10\ kvar$) to verify its feasibility. Each operating condition ($k$) relates to a corresponding displacement angle ($\delta$) as shown in Fig. 8(a). The displacement angle ($\delta$) is responsible for the power coordination between the series and shunt converters, which is realized by the online VA loading optimization techniques stated in Section IV.A. The series transformer injected voltage ($v_{se}$) and the per-phase VA loading of the shunt converter, series converter and total UPQC ($S_{sh}$, $S_{se}$, and $S_{UPQC}$) are within their rated values as presented in Fig 8(b) and (c).

TABLE III
PARAMETERS OF THE PROPOSED UPQC IN THE REAL-TIME SIMULATION

| | |
|---|---|
| Three-phase linear load | $S_{L1} = 10\ kW + j10\ kvar$<br>$S_{L2} = 6\ kW + j7\ kvar$<br>$S_{L3} = 3\ kW + j5\ kvar$<br>$S_{L4} = 2\ kW + j3\ kvar$ |
| Series converter VA rating | $S_{se\_O} = 7.3\ kVA$ |
| Shunt converter VA rating | $S_{sh\_O} = 8.8\ kVA$ |
| Series transformer VA rating | $S_{ST\_O} = 8.2\ kVA$ |
| Nominal source voltage (line voltage) | $V_{S,abc} = 400\ V$ |
| Nominal source frequency | $f_S = 50\ Hz$ |
| Voltage ratio of the series transformer | $n = 1$ |
| Series converter coupling inductance | $L_{se} = 5.0\ mH$ |
| Shunt converter coupling inductance | $L_{sh} = 2.0\ mH$ |
| dc-link capacitor | $C_{dc} = 5500\ \mu F$ |
| dc-link voltage | $V_{dc} = 700\ V$ |
| dc-link PI controller | $K_p = 0.06$, $K_i = 0.12$ |
| Sampling frequency | $f_a = 50\ kHz$ |
| Switching frequency of the converters | $f_{ch} = 10\ kHz$ |

TABLE IV
THDs OF THE SOURCE AND LOAD VOLTAGE AND CURRENT

| Three-phase nonlinear load | THD (%) | | | |
|---|---|---|---|---|
| | $v_{S,abc}$ | $v_{L,abc}$ | $i_{S,abc}$ | $i_{L,abc}$ |
| UPQC-P | 30.0 | 1.3 | 3.4 | 30.1 |
| Proposed UPQC | 30.0 | 1.3 | 3.2 | 30.1 |

## VI. REAL-TIME SIMULATION RESULTS

In recent years, the real-time simulation is increasingly used in the electrical systems due to the development of the computer technologies [32], [33]. In a real-time simulator, the performance of the designed system can be tested in real-time. The real-time simulation has shown good performance in different areas, such as HVDC systems, FACTS, modular multilevel converter, microgrids, electric ship, and so on [32], [33]. In the industrial and academic research work, the real-time simulation has been playing an essential role [32]. In this paper, the real-time simulation of the UPQC system is conducted on the OPAL-RT platform to compare the performance of the proposed UPQC system and the conventional one. The conceptual structure of the real-time simulation and the laboratory

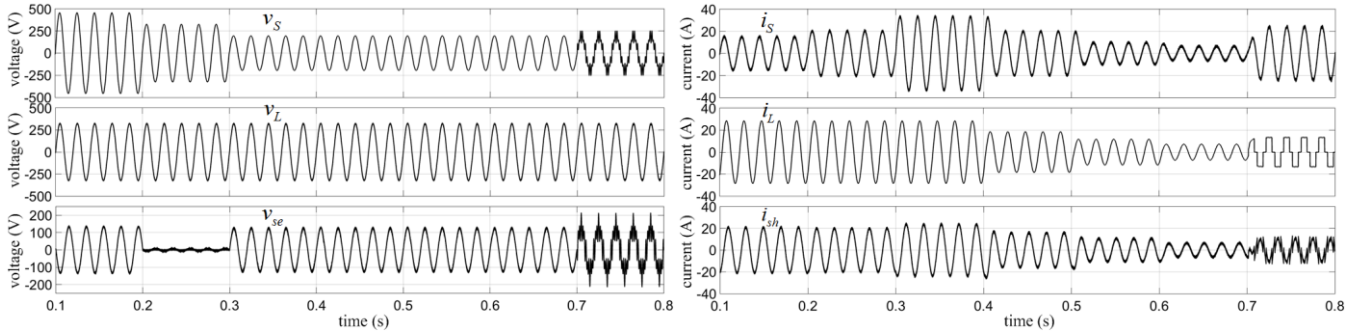


Fig. 10. Real-time simulation results of the conventional UPQC-P (a) source voltage $v_S$, load voltage $v_L$, and series transformer injected voltage $v_{se}$, (b) source current $i_S$, load current $i_L$, and shunt compensating current $i_{sh}$.

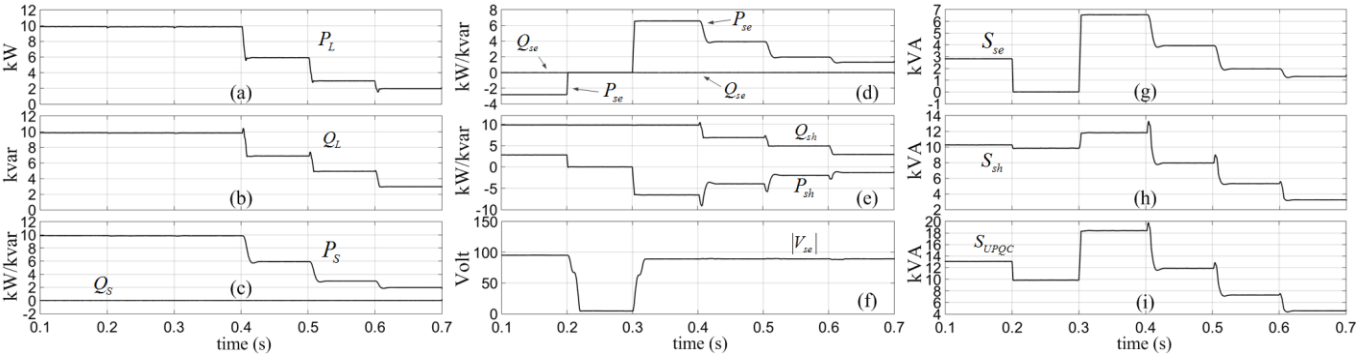


Fig. 11. Real-time simulation results of the conventional UPQC-P (a) load active power $P_L$, (b) load reactive power $Q_L$, (c) source active and reactive power $P_S$ and $Q_S$, (d) series converter active and reactive power $P_{se}$ and $Q_{se}$, (e) shunt converter active and reactive power $P_{sh}$ and $Q_{sh}$, (f) magnitude of series transformer injected voltage $|V_{se}|$, (g) series converter VA loading $S_{se}$, (h) shunt converter VA loading $S_{sh}$, and (i) total UPQC VA loading $S_{UPQC}$.

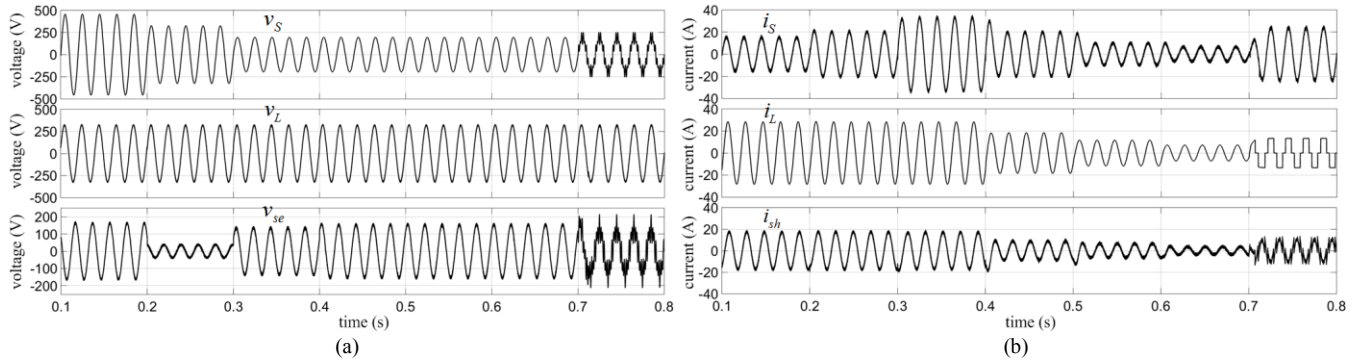


Fig. 12. Real-time simulation results of the proposed UPQC (a) source voltage $v_S$, load voltage $v_L$, and series transformer injected voltage $v_{se}$, (b) source current $i_S$, load current $i_L$, and shunt compensating current $i_{sh}$.

OPAL-RT setup are presented in Fig. 9(a) and (b), respectively. The parameters of the UPQC are summarized in Table III. By solving the nonlinear optimization problem stated in Section II, the VA ratings of the series converter, shunt converter, and series transformer are determined in Section III. The selection of the coupling inductors and the dc-link capacitor is the same as the conventional UPQC, which will not affect the size of the system. The real-time simulation results are illustrated in Figs. 10-14.

### *A. Real-Time Simulation Results of the UPQC-P*

The compensating conditions of the source and load will be introduced first. The source voltage ($v_S$) has a 40% swell during t = 0.1-0.2 s. Then it stays at steady state during t = 0.2-0.3 s. The 40% voltage sag appears at t = 0.3 s, then it continues till t = 0.8 s. The $v_S$ is also distorted during t = 0.7-0.8 s. The load power demand is $S_{L1}$ during t = 0.1-0.4 s, then it switches to $S_{L2}$, $S_{L3}$, and $S_{L4}$ at t = 0.4 s, 0.5 s, and 0.6 s, respectively. The load changes to a nonlinear load (diode rectifier connected to R-L load) during t = 0.7-0.8 s. In Fig. 10(a), The load voltage ($v_L$) remains at the desired level after compensation. The source current ($i_S$) decreases during voltage swell, increases during voltage sag, and stays constant at steady state as presented in Fig. 10(b). The THDs of the source and load voltage and current are presented in Table IV. The THDs of the $v_{L,abc}$ and $i_{S,abc}$ are within the IEEE 519 THD limitations after the compensation by UPQC-P. The results in Fig. 11 are summarized in Table V. It is noted that the source only supplies the active power and will not inject any reactive power. The series

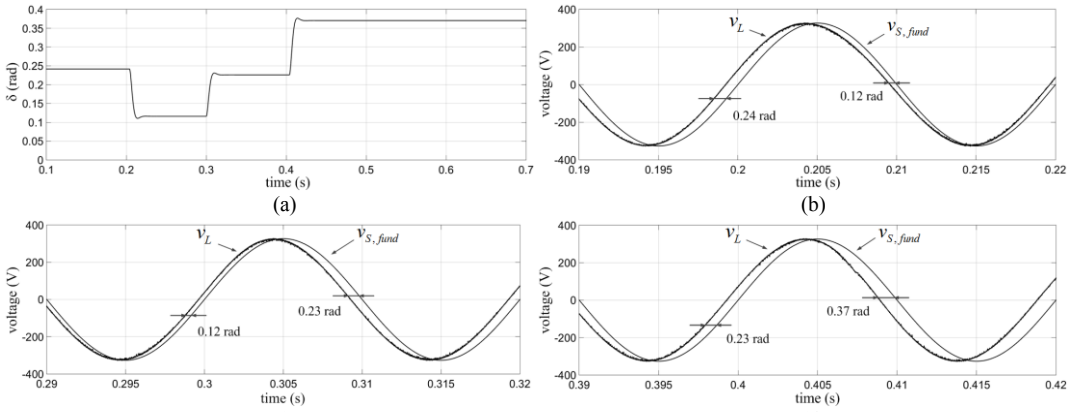


Fig. 13. Real-time simulation results of the proposed UPQC (a) displacement angle δ (rad) during t = 0.1–0.5 s, displacement angle change at (b) t = 0.2 s, (c) t = 0.3 s, and (d) t = 0.4 s.

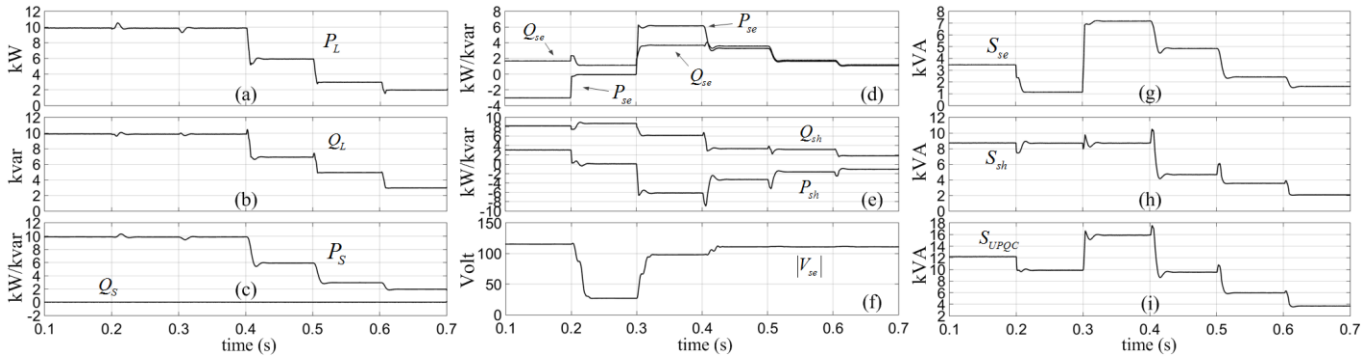


Fig. 14. Real-time simulation results of the proposed UPQC (a) load active power $P_L$, (b) load reactive power $Q_L$, (c) source active and reactive power $P_S$ and $Q_S$, (d) series converter active and reactive power $P_{se}$ and $Q_{se}$, (e) shunt converter active and reactive power $P_{sh}$ and $Q_{sh}$, (f) magnitude of series transformer injected voltage $|V_{se}|$, (g) series converter VA loading $S_{se}$, (h) shunt converter VA loading $S_{sh}$, and (i) total UPQC VA loading $S_{UPQC}$.

converter will not participate in the load reactive power compensation ($Q_{se} = 0\ kvar$). The shunt converter supported all the reactive power. The magnitude of the series transformer injected voltage ($|V_{se}|$) is 0 V at steady state, 93 V at 40% voltage swell and sag. The maximum three-phase VA loadings of the series converter, shunt converter, and total UPQC ($S_{se}$, $S_{sh}$, and $S_{UPQC}$) occur at t = 0.3-0.4 s, which are 6.6 kVA, 12.0 kVA, and 18.6 kVA.

### *B. Real-Time Simulation Results of the Proposed UPQC*

The compensating condition for the proposed UPQC is the same as that stated in Section VI.A. In Fig. 12(a), it is noted that the series converter still injects voltage ($v_{se}$) during the steady state, because the online VA loading optimization techniques compute a displacement angle ($\delta$) and send it to the reference load voltage ($v_L^*$). In Fig. 12(b), the shunt injected current ($i_{sh}$) is reduced compared with that of the UPQC-P during t = 0.1-0.7 s, which will result in a VA loading reduction in $S_{sh}$ as illustrated in Fig. 14(h). The reason is that part of the VA loading of the shunt converter is shifted to the series converter. In Fig. 14(g), it can be observed that $S_{se}$ has increased during t = 0.1-0.7 s compared with that of the UPQC-P. The power coordination is realized by the online VA loading optimization techniques stated in Section IV.A. The proposed UPQC also has the capability to deal with the distorted source voltage and

TABLE V
REAL-TIME SIMULATION RESULTS OF THE UPQC-P AND THE PROPOSED UPQC

| | Time Slot | 0.1-0.2s | 0.2-0.3s | 0.3-0.4s | 0.4-0.5s | 0.5-0.6s | 0.6-0.7s |
|---|---|---|---|---|---|---|---|
| UPQC-P | $P_L$ (kW) | 10.0 | 10.0 | 10.0 | 6.0 | 3.0 | 2.0 |
| | $Q_L$ (kvar) | 10.0 | 10.0 | 10.0 | 7.0 | 5.0 | 3.0 |
| | $P_S$ (kW) | 10.0 | 10.0 | 10.0 | 6.0 | 3.0 | 2.0 |
| | $Q_S$ (kvar) | 0.0 | 0.0 | 0.0 | 0.0 | 0.0 | 0.0 |
| | $P_{se}$ (kW) | -2.8 | 0.0 | 6.6 | 4.0 | 2.0 | 1.4 |
| | $Q_{se}$ (kvar) | 0.0 | 0.0 | 0.0 | 0.0 | 0.0 | 0.0 |
| | $P_{sh}$ (kW) | 2.8 | 0.0 | -6.6 | -4.0 | -2.0 | -1.4 |
| | $Q_{sh}$ (kvar) | 10.0 | 10.0 | 10.0 | 7.0 | 5.0 | 3.0 |
| | $S_{se}$ (kVA) | 2.8 | 0.0 | 6.6 | 4.0 | 2.0 | 1.4 |
| | $S_{sh}$ (kVA) | 10.4 | 10.0 | 12.0 | 8.0 | 5.4 | 3.3 |
| | $S_{UPQC}$ (kVA) | 13.2 | 10.0 | 18.6 | 12.0 | 7.4 | 4.7 |
| | $\|V_{se}\|$ (V) | 93 | 0 | 93 | 93 | 93 | 93 |
| Proposed UPQC | $P_L$ (kW) | 10.0 | 10.0 | 10.0 | 6.0 | 3.0 | 2.0 |
| | $Q_L$ (kvar) | 10.0 | 10.0 | 10.0 | 7.0 | 5.0 | 3.0 |
| | $P_S$ (kW) | 10.0 | 10.0 | 10.0 | 6.0 | 3.0 | 2.0 |
| | $Q_S$ (kvar) | 0.0 | 0.0 | 0.0 | 0.0 | 0.0 | 0.0 |
| | $P_{se}$ (kW) | -3.1 | -0.1 | 6.2 | 3.3 | 1.7 | 1.1 |
| | $Q_{se}$ (kvar) | 1.7 | 1.2 | 3.8 | 3.6 | 1.8 | 1.2 |
| | $P_{sh}$ (kW) | 3.1 | 0.1 | -6.2 | -3.3 | -1.7 | -1.1 |
| | $Q_{sh}$ (kvar) | 8.3 | 8.8 | 6.2 | 3.4 | 3.2 | 1.8 |
| | $S_{se}$ (kVA) | 3.5 | 1.2 | 7.3 | 4.9 | 2.5 | 1.6 |
| | $S_{sh}$ (kVA) | 8.8 | 8.8 | 8.8 | 4.7 | 3.6 | 2.1 |
| | $S_{UPQC}$ (kVA) | 12.3 | 10.0 | 16.1 | 9.6 | 6.1 | 3.7 |
| | $\|V_{se}\|$ (V) | 113 | 27 | 100 | 113 | 113 | 113 |

load current as shown in Fig. 12(a) and (b). The THDs of the $v_{L,abc}$ and $i_{S,abc}$ are within the IEEE 519 THD limitations after the compensation by the proposed UPQC as presented in Table IV.

In Fig. 13, the fundamental source voltage ($v_{S,fund}$) without sag and swell is compared with the load voltage ($v_L$) to illustrate the displacement angle ($\delta$) change. At t = 0.2 s, the $\delta$ changes from 0.24 rad to 0.12 rad. It changes to 0.23 rad at t = 0.3 s. At t = 0.4 s, it changes from 0.23 rad to 0.37 rad.

The results in Fig. 14 are summarized in Table V. It is noted that the active and reactive power of the load and source behave the same as in UPQC-P. The series converter injects the reactive power ($Q_{se}$) to share the load reactive power demand. Consequently, the reactive power from the shunt converter ($Q_{sh}$) is reduced. The maximum VA loading only appears at the full load condition. Specifically, the maximum series converter VA loading ($S_{se}$) occurs at 40% voltage sag (0.3-0.4 s), which is 7.3 kVA. The shunt converter VA loading ($S_{sh}$) maintains at 8.8 kVA during t = 0.1-0.4 s. The maximum total UPQC VA loading ($S_{UPQC}$) appears at 40% voltage sag (0.3-0.4 s), which is 16.1 kVA. The $S_{UPQC}$ is reduced compared with that of the UPQC-P at the full load condition. Furthermore, under the lower load demand conditions (t = 0.4-0.7 s), the $S_{UPQC}$ is still lower than that of the UPQC-P. The VA loadings of the proposed UPQC are within the designed VA ratings obtained in Section III.B. Under the full load condition, the magnitude of the series transformer injected voltage ($|V_{se}|$) is 27 V at steady state, 113 V at 40% voltage swell, and 100 V at 40% voltage sag. Under the lower load demand conditions, the $|V_{se}|$ is 113 V at 40% voltage sag. Obviously, the proposed UPQC system has the minimum capital cost, which is effectively reduced compared with that of the UPQC-P. Moreover, the online operating VA loading of the proposed UPQC system is simultaneously reduced due to the proposed DDC controller.

Finally, we would like to discuss the possibility of appling the proposed optimization control method in the unified power flow controller (UPFC). It is worth noting that the UPFC is operated in a power transmission system, which is at a high voltage level. The phase angle and magnitude of the bus voltage are controllable. The active and reactive power transmitted through the line can be controlled independently via controllable phase angle and bus voltage. The proposed optimization control method can be adapted for the UPFC to control the transmitted active and reactive power, while ensure the safe operation of the UPFC.

## VII. Conclusion

A generalized strategy has been proposed to determine the optimal ratings of the UPQC system, which leads to the minimum total capital cost. The DDC based controller is developed to realize the implementation of the designed UPQC system. The MATLAB and OPAL-RT simulation results validate the practicability of the proposed generalized strategy and the corresponding control method. The advantages of the proposed generalized strategy and the corresponding controller are outlined as follows:

1) Both the rating of the series transformer and those of the power converters are handled. The total capital cost is also considered, which makes the optimization process more complete and accurate.
2) The proposed generalized strategy can be utilized for the different UPQC by updating the input data according to the practical situations in different systems.
3) The DDC based controller can minimize the UPQC online VA loading and ensure the safe operation of the system.
4) The proposed generalized strategy can be extended to the advanced UPQC topologies for the future research studies.

## References


[1] M. Bollen, *Understanding Power Quality Problems: Voltage Sags and Interruptions*. Wiley-IEEE Press, 2000, pp.1-34.

[2] A. Sallam and O. Malik, *Electric Power Quality*. Wiley-IEEE Press, 2011, pp.293-318.

[3] S. Singh, B. Singh, G. Bhuvaneswari, and V. Bist, "Power factor corrected zeta converter based improved power quality switched mode power supply," *IEEE Trans. Ind. Electron*., vol. 62, no. 9, pp. 5422-5433, Sept. 2015.

[4] Z. Zheng, Y. Huan, T. Shengqing, and Z. Rongxiang, "Objective-oriented power quality compensation of multifunctional grid-tied inverters and its application in microgrids," *IEEE Trans. Power Electron*., vol. 30, no. 3, pp. 1255–1265, Mar. 2015.

[5] K. Youssef, "Power Quality Constrained Optimal Management of Unbalanced Smart Microgrids during Scheduled Multiple Transitions between Grid-Connected and Islanded Modes," *IEEE Trans. Smart Grid* , vol.PP, no.99, pp.1-1.

[6] S. Ali, K. Wu, K. Weston and D. Marinakis, "A Machine Learning Approach to Meter Placement for Power Quality Estimation in Smart Grid," *IEEE Trans. Smart Grid*, vol. 7, no. 3, pp. 1552-1561, May 2016.

[7] H. Fujita and H. Akagi, "The unified power quality conditioner: The integration of series- and shunt-active filters," *IEEE Trans. Power Electron*., vol. 13, no. 2, pp. 315–322, 1998.

[8] V. Khadkikar, "Enhancing electrical power quality using UPQC: A comprehensive overview," *IEEE Trans. Power Electron*., vol. 27, no. 5, pp. 2284–2297, May 2012.

[9] H. Hafezi, G. D'Antona, R. Faranda, D. Della Giustina, A. Dede, and G. Massa, "Power Quality Conditioning in LV Distribution Networks: Results by Field Demonstration," *IEEE Trans. Smart Grid*, vol.PP, no.99, pp.1-1.

[10] A. Mokhtarpour, M. Bathaee and H. A. Shayanfar, "Power quality compensation in smart grids with a single phase UPQC-DG," *Smart Grids (ICSG), 2012 2nd Iranian Conference on*, Tehran, 2012, pp. 1-5.

[11] J. He; Y. W. Li; C. Wang; B. Liang, "Simultaneous Microgrid Voltage and Current Harmonics Compensation Using Coordinated Control of Dual-Interfacing-Converters," *IEEE Trans. Power Electron*., vol.PP, no.99, pp.1-1

[12] G. S. Kumar, P. H. Vardhana, B. K. Kumar, and M. K. Mishra, "Minimization of VA loading of unified power quality conditioner (UPQC)," in *Proc.Power Eng., Energy Electr.Drives*, Mar. 18–20, 2009, pp. 552–557.

[13] G. S. Kumar, B. K. Kumar, and M. K. Mishra, "Power quality improvement by UPQC with minimum real power injection," *Power Electronics and Applications (EPE 2011),*Birmingham, 2011, pp. 1-10.Y. Y.

[14] Y. Y. Kolhatkar, R. R. Errabelli, and S. Das, "A slidingmode controller based optimum UPQC with minimum VA loading," in *Proc. Power Eng. Soc. Gen. Meeting*, Jun. 12–16, 2005, pp. 871–875.

[15] Y. Y. Kolhatkar and S. Das, "Experimental investigation of a single-phase UPQC with minimum VA loading," *IEEE Trans. Power Del*., vol. 22, no. 1, pp. 371–380, Jan. 2007.

[16] M. Basu, S. Das, and G. Dubey, "Comparative evaluation of two models of UPQC for suitable interface to enhance power quality," *Elect. Power Syst. Res.*, vol. 77, no. 7, pp. 821–830, 2007.

[17] M. Basu, M. Farrell, F. Conlon, K. Gaughan, and E. Coyle, "Optimal control strategy of UPQC for minimum operational losses," in *Proc. 39th Int. Univ. Power Eng*., Sep. 6–8, 2004, pp. 246–250.

[18] M. Basu, S. Das, and G. Dubey, "Investigation on the performance of UPQC-Q for voltage sag mitigation and power quality improvement at a critical load point," *Inst. Eng. Technol. Gen., Transm. Distrib*., vol. 2, no. 3, pp. 414–423, May 2008.
[19] W. C. Lee, D. M. Lee, and T. K. Lee, "New control scheme for a unified power-quality compensator-Q with minimum active power injection," *IEEE Trans. Power Del*., vol. 25, no. 2, pp. 1068–1076, Apr. 2010.
[20] B. B. Ambati and V. Khadkikar, "Optimal Sizing of UPQC Considering VA Loading and Maximum Utilization of Power-Electronic Converters," *IEEE Trans. Power Del*., vol.29, no.3, pp.1490-1498, Jun. 2014.
[21] V. Khadkikar and A. Chandra "A new control philosophy for a unified power quality conditioner (UPQC) to coordinate load-reactive power demand between shunt and series inverters," *IEEE Trans. Power Del*., vol. 23, no. 4, pp.2522 -2534 2008.
[22] V. Khadkikar and A. Chandra, "UPQC-S: a novel concept of simultaneous voltage sag/swell and load reactive power compensations utilizing series inverter of UPQC," *IEEE Trans. Power Electron*., vol. 26, no. 9, pp. 2414–2425, Sep. 2011.
[23] S. Yin, X. W. Li, H. J. Gao, and O. Kaynak, "Data-based techniques focused on modern industry: An overview," *IEEE Trans. Ind. Electron*., vol. 62, no. 1, pp. 657–667, Jan. 2015.
[24] Z. S. Hou and Z. Wang, "From model-based control to data-driven control: Survey, classification and perspective," *Inf. Sci*., vol. 235, pp. 3–35, 2013.
[25] H. Zhang; J. Zhou; Q. Sun; J. M. Guerrero; D. Ma, "Data-Driven Control for Interlinked AC/DC Microgrids Via Model-Free Adaptive Control and Dual-Droop Control," *IEEE Trans. Smart Grid* , vol.PP, no.99, pp.1-15.
[26] Y. Jia; T. Chai, "A Data-Driven Dual-Rate Control Method for a Heat Exchanging Process," *IEEE Trans. Ind. Electron*., vol.PP, no.99, pp.1-1.
[27] D. Xu, B. Jiang and F. Liu, "Improved data driven model free adaptive constrained control for a solid oxide fuel cell," *IET Control Theory Appl*., vol. 10, no. 12, pp. 1412-1419, 2016.
[28] K. Sindhya, K. Miettinen, and K. Deb, "A hybrid framework for evolutionary multi-objective optimization," *IEEE Trans. Evol. Comput.*, vol. 17, no. 4, pp. 495–511, Aug. 2013.
[29] R. H. Byrd, M. E. Hribar, and J. Nocedal, "An interior point algorithm for large-scale nonlinear programming," *SIAM J. Opt*., vol. 9, no. 4, pp. 877–900, 1999.
[30] H. Akagi, E. Watanabe, and M. Aredes, *Instantaneous Power Theory and Applications to Power Conditioning*. Hoboken, NJ, USA: Wiley, 2007, ser. IEEE Press Series on Power Engineering.
[31] R. A. Modesto, S. A. O. da Silva, A. A. de Oliveira and V. D. Bacon, "A Versatile Unified Power Quality Conditioner Applied to Three-Phase Four-Wire Distribution Systems Using a Dual Control Strategy," *IEEE Trans. Power Electron*., vol. 31, no. 8, pp. 5503-5514, Aug. 2016.
[32] X. Guillaud et al., "Applications of Real-Time Simulation Technologies in Power and Energy Systems," *IEEE Power and Energy Technology Systems Journal*, vol. 2, no. 3, pp. 103-115, Sept. 2015.
[33] P. Venne, J. N. Paquin, and J. Bélanger, "The what, where and why of real-time simulation," in *Proc. PES General Meeting*, Oct. 2010, pp. 37–49.

**Jian Ye** (S'15) received the B.Eng. degree in electrical engineering from Wuhan University, Wuhan, China, in 2012, and the M.Sc. degree from Nanyang Technological University, Singapore, in 2013, where he is currently working towards the Ph.D. degree at the School of Electrical and Electronic Engineering.

His research interests include power electronics for various applications such as connecting renewable energy sources, energy devices to microgrids, and power quality compensation.

**H. B. Gooi** (SM'95) received the B.S. degree in EE from National Taiwan University in 1978; the M.S. degree in EE from the University of New Brunswick in 1980; and the Ph.D. degree in EE from Ohio State University in 1983.

From 1983 to 1985, he was an Assistant Professor with Lafayette College, Easton. From 1985 to 1991, he was a Senior Engineer with Empros (now Siemens), Minneapolis, where he was responsible for the design and testing coordination of domestic and international energy management system projects. In 1991, he joined the School of Electrical and Electronic Engineering, Nanyang Technological University, Singapore, as a Senior Lecturer, where he has been an Associate Professor since 1999. He was the Deputy Head of Power Engineering Division during 2008-2014. His current research interests include microgrid energy management systems, electricity markets, spinning reserve, energy efficiency, and renewable energy sources.

**Fengjiang Wu** (M'15) received the B.S., M.S. and Ph.D. degrees in electrical engineering from Harbin Institute of Technology (HIT), Harbin, China, in 2002, 2004 and 2007, respectively.

Since 2007, he has been with the Department of Electrical Engineering, HIT, where he is currently an Associate Professor. Since 2016, he has been in the School of Electrical and Electronic Engineering, Nanyang Technological University, Singapore (a Senior Research Fellow). His research interests include renewable energy generation, microgrids, multilevel inverter technology and electric machines drives.